Nanoscale

PAPER

View Article Online
View Journal | View Issue

Cite this: *Nanoscale*, 2014, **6**, 13817

Nitrogen and sulfur co-doped carbon dots with strong blue luminescence†

Hui Ding, Ji-Shi Wei and Huan-Ming Xiong*

Received 28th July 2014,
Accepted 13th September 2014

DOI: 10.1039/c4nr04267k

www.rsc.org/nanoscale

Sulfur-doped carbon dots (S-CDs) with a quantum yield (QY) of 5.5% and nitrogen, sulfur co-doped carbon dots (N,S-CDs) with a QY of 54.4% were synthesized, respectively, *via* the same hydrothermal route using α-lipoic acid as the carbon source. The obtained S-CDs and N,S-CDs had similar sizes but different optical features. The QY of N,S-CDs was gradually enhanced when extending the reaction time to increase the nitrogen content. After careful characterization of these CDs, the doped nitrogen element was believed to be in the form of C=N and C–N bonds which enhanced the fluorescence efficiency significantly. Meanwhile, the co-doped sulfur element was found to be synergistic for nitrogen doping in N,S-CDs. The optimal N,S-CDs were successfully employed as good multicolor cell imaging probes due to their fine dispersion in water, excitation-dependent emission, excellent fluorescence stability and low toxicity. Besides, such N,S-CDs showed a wide detection range and excellent accuracy as fluorescent sensors for Fe^{3+} ions.

1. Introduction

Carbon dots (CDs), as a new type of photoluminescent (PL) nanomaterial, have received much attention due to their low cost, outstanding biocompatibility and unique physical properties in the last decade.[1,2] Scientists have produced various CDs by both top-down methods and bottom-up strategies,[3–7] and applied them in many fields.[8–12] For example, CDs synthesized *via* an electrochemical method were used to prepare highly efficient catalysts for photodegradation of methyl blue;[5] strongly luminescent CDs produced by a hydrothermal method were applied for multicolor patterning, Fe^{3+} detection and cell imaging;[10] nitrogen-rich CDs prepared by emulsion-templated carbonization were dispersed into a polymer matrix to fabricate luminescent films for lighting systems.[13] Among these unique properties of CDs, PL is the most amazing because CDs' fluorescence heavily depends on the excitation conditions and the raw materials, which is distinguished from other semiconductor nanoparticles.[14,15] The raw materials for CDs vary from organic chemicals used in the lab to natural biomaterials like soy milk,[16] orange juice[17] and hair fibers.[18] CDs of the same size but made from different raw materials always exhibit quite different PL phenomena.[19] Therefore, controlling the compositions and structures of CDs is a key to understand their complicated luminescence mechanisms.

By doping CDs with other non-metallic elements it is possible to adjust their compositions and structures. For instance, Zhang *et al*. prepared N-doped CDs with tunable luminescence by adjusting N contents;[20] Qian *et al*. improved the QY of CDs by incorporating nitrogen and speculated that the fluorescence enhancement originated from the polyaromatic structures induced by the doped nitrogen.[21] Sun *et al*. prepared highly luminescent N-doped carbon dots with their QY up to 94% and ascribed the high yield of radiative recombination between the trapped electrons and holes to a newly formed surface state induced by the nitrogen in CDs.[22] By far, plenty of work have been focused on the nitrogen doped CDs, but the CDs containing a sulfur dopant[23] and co-dopants[24] have been rarely reported. In addition, although nitrogen doping is usually found to enhance CD fluorescence,[21] the corresponding mechanisms remain unclear. Thus, it is a challenge to study the synergistic effects of the two dopants and, meanwhile, search for the origin of the luminescence enhancement by controlling the CD composition.

In the present work, we compared the sulfur-doped CDs and the nitrogen, sulfur co-doped CDs with similar particle sizes. Both of them were synthesized *via* the one-step hydrothermal route using α-lipoic acid as the carbon source, but their fluorescence properties were quite different. After careful characterization, C=O groups on the CD surface were considered as the main emission centers for blue luminescence, while C=N and C–N bonds in the form of polyaromatic

Department of Chemistry and Shanghai Key Laboratory of Molecular Catalysis and Innovative Materials, Fudan University, Shanghai 200433, P. R. China.
E-mail: hmxiong@fudan.edu.cn

† Electronic supplementary information (ESI) available: Experimental details and comparable characterization of three kinds of CDs. See DOI: 10.1039/c4nr04267k

structures were proved to be the key factors for promoting the fluorescence of N,S-CDs. The sulfur atoms existing in N,S-CDs were confirmed to be synergistic for doping nitrogen in CDs. The obtained N,S-CDs exhibited strong blue emission with a QY of 54.4%, low cytotoxicity, high sensitivity towards Fe^{3+} ions and multicolor imaging function for the living cells.

2. Experimental section

2.1. Synthesis of S-CDs and N,S-CDs

For sulfur-doped carbon dots (S-CDs), 0.1 g of NaOH was dissolved in 50 ml of DI-water to obtain a basic solution. Then 0.5 g of α-lipoic acid was added and stirred to obtain a pale yellow solution. After that, the solution was transferred into a poly(*para*-phenol)-lined stainless steel autoclave and heated at 250 °C for 1, 3, 7, 11, 15 and 19 hours. After cooling down to room temperature, the obtained solution was purified *via* dialysis through an analysis membrane (Spectrum, MW cutoff 3500). For nitrogen and sulfur co-doped carbon dots (N,S-CDs), 0.5 g of α-lipoic acid, 0.1 g of sodium hydroxide and 0.3 g of ethylenediamine were added to 50 ml of H_2O and then stirred to obtain a pale yellow solution. The subsequent treatments were the same as those for S-CDs. Finally, two CD aqueous solutions were freeze-dried for characterization.

2.2. Synthesis of N-CDs

0.5 g of 3-cyclopentylpropionic acid and 0.3 g of ethylenediamine were dissolved in 50 ml of pure water. Then, 0.1 g of sodium hydroxide was also added. The obtained colorless transparent solution was treated in the same way as those for S-CDs.

2.3. Reduction of N,S-CDs

An excess of $NaBH_4$ was added to N,S-CD aqueous solution and the mixture was stirred at room temperature for 4 h. After the reaction, the product was transferred into a dialysis bag and dialyzed for 2 days.

2.4. Fluorescent sensors for Fe^{3+} detection

The freeze-dried N,S-CD powder was dissolved in a PBS solution (pH = 7.4) with a concentration of 0.1 mg mL^{-1}. Then, aqueous solutions containing thirteen kinds of metal ions, Na^+, K^+, Sn^{4+}, Cu^{2+}, Zn^{2+}, Fe^{3+}, Ba^{2+}, Mg^{2+}, Co^{2+}, Fe^{2+}, Ca^{2+}, Al^{3+} and Pb^{2+}, were prepared, respectively, with a concentration of 1 mM. To evaluate the selectivity of N,S-CDs, 100 μL of the above metal ion solution was mixed with 900 μL of the N,S-CD solution, and then the PL spectra were measured for recording the fluorescence intensity. To evaluate the detection range of Fe^{3+}, 100 μL of the solutions containing different concentrations of Fe^{3+} were mixed with 900 μL of the N,S-CD solution, respectively. The control sample was prepared by mixing 100 μL of pure water with 900 μL of the N,S-CD solution. All the samples were excited at 390 nm, and the intensities of fluorescence emission at 472 nm for each sample were recorded for comparison.

2.5. Cytotoxicity assay

HeLa cells were seeded in a 96-well cell culture plate in Dulbecco's modified Eagle medium (DMEM) at a density of 5×10^4 cells mL^{-1} with 10% fetal bovine serum (FBS) at 37 °C and with 5% CO_2 for 24 h. Afterwards, the culture medium was replaced with 200 μL of DMEM containing the carbon dots at different doses and cultured for another 48 h. Then, 20 μL of 5 mg mL^{-1} MTT (3-(4,5-dimethylthiazol-2yl)-2,5-diphenyltetrazolium bromide) solution was added to every cell well. The cells were further incubated for 4 h, followed by removal of the culture medium with MTT, and then 150 μL of DMSO was added. The resulting mixture was shaken for 15 min at room temperature. The absorbance of MTT at 492 nm was measured on an automatic ELISA analyzer (SPR-960). The control data were obtained in the absence of CDs. Each experiment was conducted 5 times and the average data were presented.

2.6. Multicolor cell imaging

Cellular fluorescent images were recorded using a Leica Tcs sp5 Laser Scanning Confocal Microscope. HeLa cells were seeded in 6-well culture plates at a density of 10^5 per well in DMEM containing 10% fetal bovine serum (FBS) at 37 °C in a 5% CO_2 incubator for 24 h. After removing DMEM, the mixture of N,S-CDs (100 μg mL^{-1}) in the DMEM medium was added into each well for 2 h of incubation. Finally, the cells were washed twice with phosphate buffer solution (PBS) to remove extracellular CDs and were then fixed with 4% paraformaldehyde.

2.7. Quantum yield (QY) measurements

The quantum yield (QY) was measured using an integrating sphere attached to a Horiba Jobin Yvon fluoromax-4 spectrofluorometer. Firstly, the aqueous solution of N,S-CDs was diluted to keep the absorption intensity below 0.1 at the best excitation wavelength of 390 nm. Subsequently, the aqueous solution was added into a 10 mm fluorescence cuvette, placed in the integrating sphere and excited with monochromatic light of 390 nm. We recorded the fluorescence spectrum of our sample in the ranges of 380–400 nm and 405–750 nm, respectively. Meanwhile, we also recorded the same fluorescence spectrum of pure water under the same conditions. Finally, we used the fluorescent software to calculate the QY of our samples. Each experiment was conducted three times in parallel and the average value of QY was calculated. Besides, QY of N-CDs was also tested with the same conditions because of their similar PL spectra. In addition, we recorded the fluorescence spectrum of S-CDs in the ranges of 360–380 nm and 385–720 nm, respectively, because the best excitation wavelength for S-CDs was 370 nm. The other measurement conditions were the same as those for N,S-CDs.

3. Results and discussion

3.1. Characterization of S-CDs and N,S-CDs

S-CDs were obtained by hydrothermal treatment on the basic aqueous solution of α-lipoic acid in poly(*para*-phenol)-lined stainless steel autoclaves at 250 °C for different times and then purified by dialysis against water. In the case of N,S-CDs, ethylenediamine was added to the same reaction systems together with α-lipoic acid, as illustrated in Scheme S1.† All the samples selected for characterization were prepared at 250 °C for 19 hours, except those specially pointed out.

The transmission electron microscopy (TEM) images (Fig. 1) show that the S-CDs and N,S-CDs are uniform and well dispersed with an average diameter of 2.5 and 2.7 nm, respectively (see Fig. S1†). The high-resolution TEM (HRTEM) image of S-CDs in Fig. 1 shows the well-resolved lattice fringes with an average interplanar spacing of 0.32 nm, which is very close to the (002) diffraction facets of graphite.[24] Meanwhile, a similar value of 0.34 nm is found in N,S-CDs, indicating that both S-CDs and N,S-CDs have completed graphitization during reactions.[25] X-ray diffraction measurements show that both samples have the same diffraction peak at around 23.1°, corresponding to an interlayer spacing of 0.38 nm. This value is a little larger than the result of HRTEM, owing to the existence of organic functional groups on CD surfaces (Fig. S2†).[2,26]

The Raman spectra of the two CDs (Fig. S3†) show two peaks centered at 1351 and 1576 cm^{-1}, representing D and G bands of the carbon material, respectively.[27,28] The intensity ratios I_D/I_G referring to the ratio between the disordered structure and the graphitic structure are 0.93 and 0.86, respectively, for S-CDs and N,S-CDs, indicating that S-CDs are more disordered and amorphous than N,S-CDs.[2,29] The higher graphitic extent of N,S-CDs may result from the polyaromatic structures induced by the incorporated nitrogen atoms and the protonation of nitrogen atoms on CD surfaces.[21,30] The Raman results suggest that both CDs consist of graphitic sp2 carbon atoms in the crystalline cores and sp3 carbon defects on the surfaces or in the cores.[27,31]

The Fourier transform infrared (FT-IR) spectra of S-CDs and N,S-CDs (Fig. 2) show the absorption bands at around 3420, 1562 and 2928 cm^{-1}, corresponding to the stretching vibrations of O–H/N–H, C=C and C–H, respectively.[18,29,32] Both samples have similar IR bands within the range of 1000–1400 cm^{-1}, which are attributed to the stretching vibrations of C–O, C–S and C–H, respectively.[24,33] However, the C=O stretching vibration band at 1705 cm^{-1} in S-CDs shifts to 1670 cm^{-1} in the N,S-CDs, and a new band at 1122 cm^{-1} arises for the asymmetric stretching vibrations of C–NH–C, which confirms that ethylenediamine molecules are graphed onto the N,S-CD surfaces through amide bonds.[10,33] Moreover, other two bands at 1640 and 1443 cm^{-1}, representing the typical stretching modes of C=N and C–N, respectively, in heterocycles, are only observed in N,S-CDs,[34,35] suggesting that nitrogen atoms not only exist on the particle surface in the form of amide bonds but also exist in the cores as polyaromatic structures.

The X-ray photoelectron spectra (XPS) are employed to investigate the surface states of S-CDs (Fig. S4†) and N,S-CDs (Fig. 3). The wide spectrum of N,S-CDs (Fig. 3a) shows four typical peaks of C 1s (285 eV), N 1s (400 eV), O 1s (531 eV) and

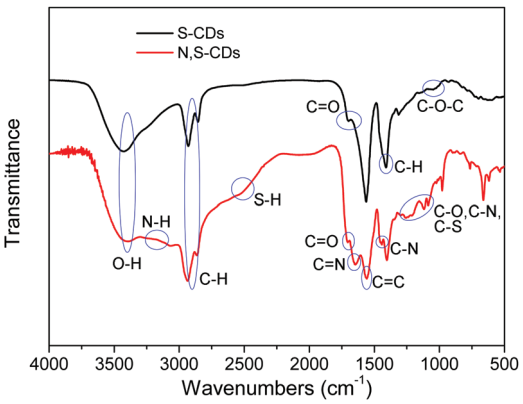

Fig. 2 FT-IR spectra for S-CDs and N,S-CDs.

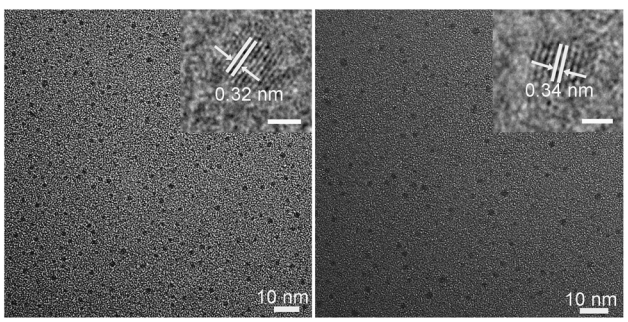

Fig. 1 TEM and HRTEM (inset) images of the as-prepared S-CDs (left) and N,S-CDs (right). The scale bar represents 2 nm in the inset images.

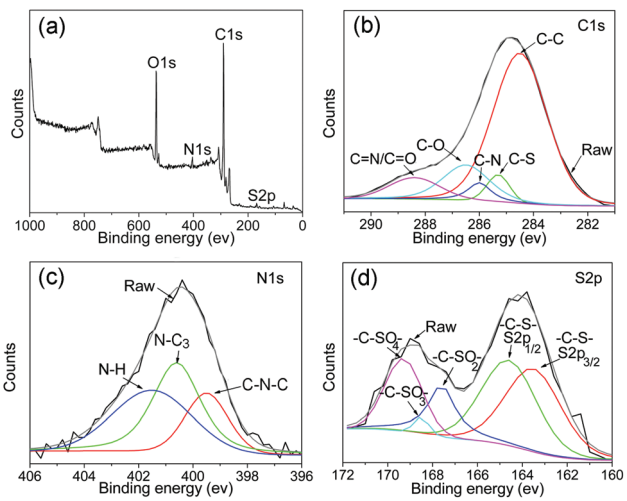

Fig. 3 (a) XPS spectra of the obtained N,S-CDs. (b–d) High-resolution XPS spectra of the C 1s, N 1s and S 2p of the N,S-CDs, respectively.

S 2p (164 eV).[18,24] The high-resolved C 1s XPS spectrum (Fig. 3b) can be deconvoluted into five peaks at 284.5, 285.3, 286.0, 286.5 and 288.2 eV, which represent C 1s states in C–C/C=C, C–S, C–N, C–O and C=O/C=N bonds, respectively.[11,18] The N 1s spectrum (Fig. 3c) displays three peaks at 399.5, 400.6 and 401.6 eV, which can be ascribed to pyridinic C–N–C, pyrrolic C_2–N–H and graphitic N–C_3,[21] respectively. The S 2p spectrum (Fig. 3d) confirms two main bands at 164.0 and 167.6 eV, which confirms sulfur in two groups of –C–S– and –C–SO_x–, respectively. The former can be resolved into two peaks at 163.5 and 164.6 eV, which are assigned to the $2p_{3/2}$ and $2p_{1/2}$ of the –C–S– covalent bond, respectively.[18] The latter can be deconvoluted into three peaks at 167.6, 168.5 and 169.3 eV, owing to –C–SO_x– (x = 2, 3, 4) species, respectively.[36] The S 2p spectrum of N,S-CDs is similar to that of S-CDs (Fig. S4d†), while the N 1s spectrum of N,S-CDs proves the newly formed polyaromatic structures containing C–N and C=N, in accord with the FTIR analyses.

3.2. Blue luminescence of N,S-CDs

The UV-visible absorption and fluorescence spectra of the S-CDs and N,S-CDs are compared in Fig. 4. In Fig. 4b, both samples exhibit a similar absorption onset at 320 nm due to the trapping of excited-state energy by the surface states,[24,37] but only N,S-CDs have a clear absorption peak at 270 nm, which may be ascribed to the π–π* transition of C=N bonds.[8,31,38] In Fig. 4c and d, both samples exhibit the typical CD fluorescence which depends on the excitation wavelength.[25] However, N,S-CDs show much stronger blue emission than S-CDs (Fig. 4a), and its QY is up to 54.4%, much higher than that of S-CDs (5.5%). Such a strong fluorescence is ascribed to the nitrogen doping undoubtedly.

Although the fluorescence mechanisms for CDs are controversial at present, many researchers agree that quantum effects,[2,39] surface states[24,31] and carbogenic cores[10,40] are the main factors that determine the emission features of CDs. In the present research, since S-CDs and N,S-CDs have similar particle sizes, the quantum effects can be excluded from comparison. It is known that the composition of the CDs greatly influences the surface states and carbogenic cores of CDs,[24,41,42] so first we studied CD performances by changing their composition. For this purpose, both S-CDs and N,S-CDs are collected at different reaction times and measured by spectroscopy techniques. In Fig. S5 and S6,† the UV-Vis absorption and fluorescence spectra of the S-CDs synthesized at different times show almost no changes, indicating that the reaction time does not affect the optical properties of S-CDs significantly. In contrast, the absorption spectra of N,S-CDs (Fig. S7†) show a featured peak at 270 nm that increases gradually along with the reaction time, which means that more and more C=N bonds are produced in this process.[25,38] In the meantime, the blue emission at about 472 nm becomes stronger and stronger (Fig. S8†), and the main emission peak for N,S-CDs redshifts from 422 nm to 472 nm (Fig. S9†). According to the elemental analyses (Table S1†) and XPS results (Table S2†), extending the reaction time can improve the nitrogen doping extent, and produce more C–N, and C=N/C=O bonds. Hence, these newly formed bonds are definitely responsible for the strong blue emission. As a result, the QY of N,S-CDs increases along with the nitrogen content (Fig. S10 and S11†), while the QY of S-CDs shows almost no changes when extending the reaction time.

To further investigate the origin of the CD fluorescence, the fluorescence lifetime of both S-CDs and N,S-CDs are measured and compared in Fig. 5, Fig. S12 and Table S3,† respectively. The fluorescence decay curves of all CD samples can be fitted by a double-exponential formula,[29] involving the lifetimes τ_1 and τ_2. For S-CDs, τ_1 is about 1.5 ns while τ_2 is about 3.8 ns, and their proportions are 43% and 57%, respectively. For N,S-CDs, τ_1 is about 2 ns while τ_2 is about 6 ns, independent of the reaction time. However, the lifetime proportion of N,S-CDs changes continuously when extending the reaction time.

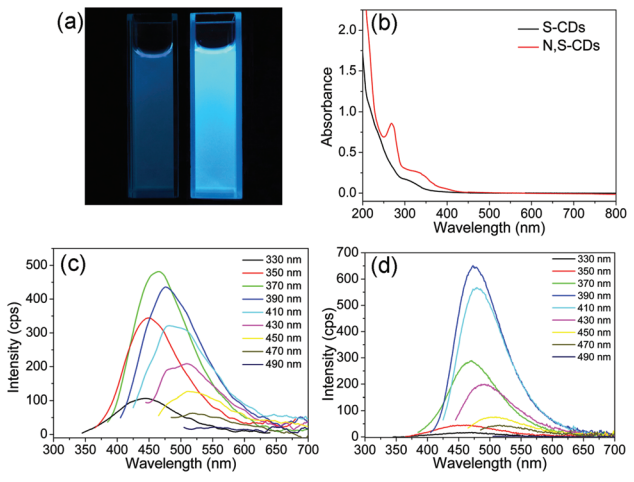

Fig. 4 (a) A photo of the obtained S-CDs (left) and N,S-CDs (right) under UV light (365 nm). (b) UV-visible absorption spectra of the S-CDs and N,S-CDs. (c, d) Fluorescence spectra of the S-CDs and N,S-CDs under different excitation conditions.

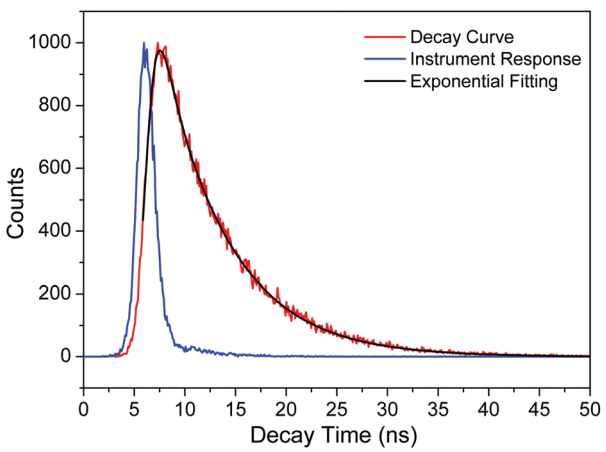

Fig. 5 Fluorescence lifetime of N,S-CDs measured by monitoring the emission at 472 nm when excited at 390 nm.

On one hand, the average lifetime for N,S-CDs is longer than that of S-CDs, and increases gradually with extending reaction time, which means that nitrogen doping in CDs produces more luminescent centers.[43] On the other hand, the τ_2 proportion increases from 60.6% to 91.5% as the reaction time prolongs from 1 h to 19 h, indicating that τ_2 is directly related to the N content and dominates the fluorescence properties of N,S-CDs. To further verify this point, we compare the transient fluorescence spectra of the τ_2 at 6.54 ns collected using a fluorescence lifetime spectrometer (QM40) and the steady-state fluorescence spectra collected using a Horiba Jobin Yvon fluoromax-4 spectrofluorometer in Fig. S13.† Both PL emission curves overlay with each other, so that C=N and C–N bonds are confirmed to be the origin of the enhanced QY of N,S-CDs.

It is known that sodium borohydride ($NaBH_4$) can selectively reduce some functional groups like C=N and C=O on CD surfaces.[31,44] In Fig. 6a, absorption spectra clearly display a decrease at 320 nm after $NaBH_4$ treatment, indicating that C=O functional groups are mostly reduced. But another absorption peak at 270 nm shows almost no change after $NaBH_4$ treatment, suggesting that C=N bonds mainly exist in carbon cores.[21,33] The FT-IR spectra of the reduced N,S-CDs (Fig. 6b) still have clear absorption at 1640 (C=N) and 1443 (C–N) cm^{-1}, respectively, in accord with the UV-Vis absorption spectra. Fig. 6c and 6d show that after C=O reduction, the maximum emission wavelength blue shifts from 470 nm to 410 nm,[45] while the QY of the reduced N,S-CDs is still as high as 45.9% when excited with 390 nm light, hence the high fluorescence efficiency of N,S-CDs is mainly ascribed to the C=N and C–N bonds that existed in CD cores. According to the above analyses, we conclude that both C=O groups on the surfaces and the C=N/C–N bonds in CD cores are responsible for the blue emission of N,S-CDs, but the latter dominates when more and more nitrogen atoms are doped into CDs.

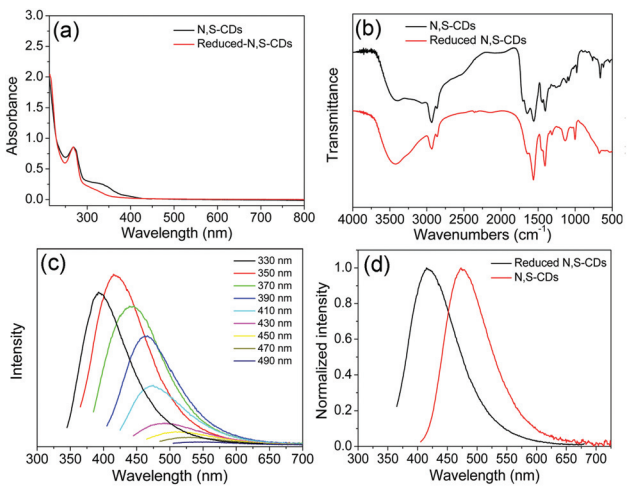

Fig. 6 (a) Absorption spectra of the N,S-CDs and the reduced N,S-CDs. (b) FT-IR spectra of the N,S-CDs (upper) and the reduced N,S-CDs (lower). (c) Fluorescence spectra of the reduced N,S-CDs. (d) The maximum emission peaks of the N,S-CDs and the reduced N,S-CDs.

3.3. Synergistic role of sulfur atoms

In order to disclose the sulfur functions, nitrogen-doped carbon dots (N-CDs) were specially synthesized using 3-cyclopentylpropionic acid and ethylenediamine as starting materials and a similar route as shown in Scheme S2.† Such N-CDs are monodispersed in water and have an average size of 2.6 nm (Fig. S14†), which is very close to that of N,S-CDs, suggesting that the quantum effects can be ignored in comparison.[31,39] In the UV-Vis absorption spectra of such N-CDs (Fig. S16†), N-CDs also exhibit two absorption bands at 270 and 320 nm, owing to C=N and C=O bonds, respectively.[46] But N-CDs exhibit much lower absorption at 270 nm than N,S-CDs, indicating the lower content of C=N bonds in N-CDs. The PL spectra (Fig. S15†) show that the maximum emission at 472 nm is obtained by excitation at 390 nm, implying that the fluorescent centers of N-CDs are similar to those of N,S-CDs.[24,47] Besides, the absorption spectra and PL spectra for the N-CDs synthesized by extending the reaction time are recorded in Fig. S17 and S18,† respectively. Both the characteristic UV-Vis absorption band at 270 nm and the characteristic PL emission band at 472 nm increase gradually when prolonging the reaction time, confirming that more and more nitrogen elements are doped into CDs. The QY evolution curves of S-CDs, N-CDs and N,S-CDs are compared in Fig. S10.† Although the three curves display a similar increasing trend until the highest QY, the optimal QY of N-CDs is 20.1%, which is lower than 54.4% of N,S-CDs but higher than 5.5% of S-CDs. Therefore, we confirm that the co-doped sulfur atoms in N,S-CDs can help enhance the effect of nitrogen doping in a synergistic role.[24] It has been reported that the sulfur and nitrogen co-doped carbon materials exhibit higher catalytic activity towards the oxygen reduction reaction in comparison with the nitrogen-doped carbon materials through a cooperative effect.[48–50] In addition, DFT calculations revealed that the synergistic enhancement of the CD performances was from the redistribution of spin and charge densities after the dual doping of S and N atoms.[48] In our work, sulfur atom doping gives CDs more opportunities to form C=N bonds, as confirmed by the enhanced absorption at 270 nm. Thus, we think that redistribution of spin and charge densities in the CDs is the basis of synergetic effects.

3.4. Fe^{3+} detection and multicolor cell imaging

Fe^{3+} is an important metal ion in life because of its essential functions in oxygen transport, oxygen metabolism, electronic transfer and many catalytic processes.[10,51] Fe^{3+} ions can be detected with CDs *via* luminescence measurements, but those published results suffered from the narrow ranges of detection concentrations,[51,52] weak accuracy[33] or low selectivity.[10] Fig. 7a shows the original N,S-CDs before and after quenching by Fe^{3+}. In comparison with many common metal ions (Fig. 7b), only Fe^{3+} is able to quench the fluorescence of the N,S-CDs. Such a specific fluorescence quenching effect may originate from the strong interactions between Fe^{3+} ions and the surface groups of N,S-CDs which transfer the photoelectrons from CDs

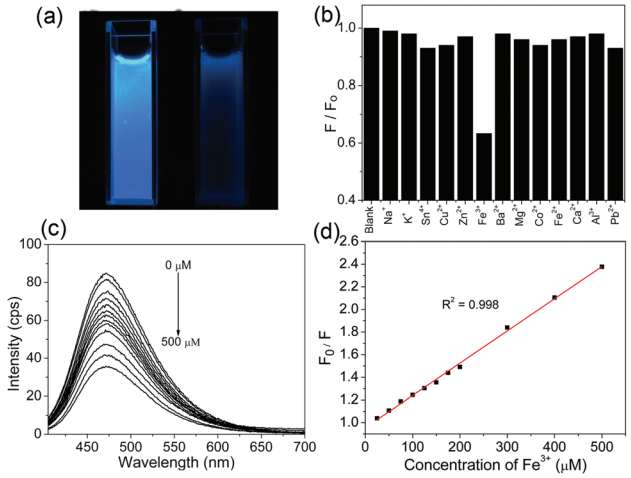

Fig. 7 (a) A photo of the aqueous solutions of N,S-CDs without (left) and with (right) 300 μM of Fe^{3+}. (b) Comparison of fluorescence intensities of N,S-CDs after adding different metal ions with the same concentration of 100 μM. (c) Fluorescence spectra of the N,S-CDs mixed with various concentrations of Fe^{3+}: 0, 25, 50, 75, 100, 125, 150, 175, 200, 300, 400 and 500 μM from top to bottom. (d) The emission intensity ratio F_0/F depends on the concentrations of the added Fe^{3+}, which is derived from the results in (c). F_0/F ratios are evaluated by the emission at 472 nm, and the excitation wavelength is set at 390 nm.

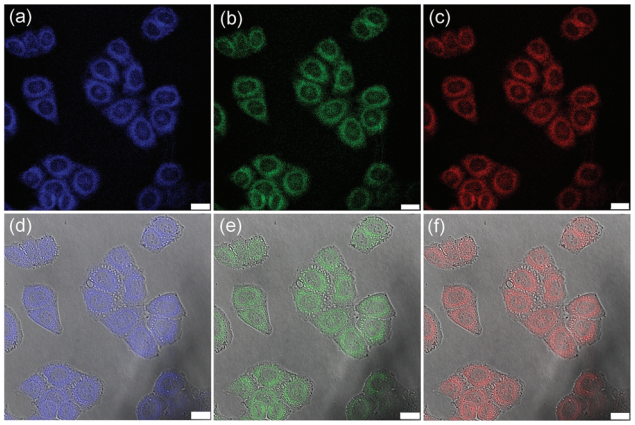

Fig. 8 Confocal fluorescence images of HeLa cells after incubation with N,S-CDs (100 μg mL^{-1}) for 2 h. These images are obtained by (a) 405 nm excitation and the emission is recorded at 420–520 nm, (b) 458 nm excitation and the emission is recorded at 500–585 nm and (c) 514 nm excitation and the emission is recorded at 575–670 nm. The images (d–f) are the merged images of (a–c) with the corresponding bright field graphs. All scale bars represent 25 nm.

to Fe^{3+} ions.[10,33] The fluorescence spectra of the N,S-CD solution containing different concentrations of Fe^{3+} are measured at the excitation wavelength of 390 nm (Fig. 7c). The ratios of F_0/F have a good linear correlation with the Fe^{3+} concentrations in the range of 25–500 μM (Fig. 7d), much larger than those of recently reported values.[10,33,51,52] Here F_0 and F are the fluorescent intensities of CDs at 472 nm in the absence and presence of Fe^{3+} ions, respectively. The quenching efficiency is fitted by the Stern–Volmer equation, $F_0/F = 1 + K_{SV}[Q]$, where K_{SV} is the Stern–Volmer quenching constant and [Q] is the Fe^{3+} concentration.[28] The K_{SV} value is calculated to be 2.85×10^3 L mol^{-1} with a correlation coefficient R^2 of 0.998. The detection limit is estimated to be 4 μM at a signal-to-noise ratio of 3.[53] The above results clearly prove that our CDs are very promising for Fe^{3+} detection in practical applications.

Before biological application, the fluorescence stability of N,S-CDs at different pH values and ionic strengths, long-time irradiation of UV or storage under ambient conditions, have been measured and illustrated in Fig. S20.† All the results prove that our N,S-CDs are very stable for practical application. The cytotoxicity toward HeLa cells is performed by the conventional MTT assay (Fig. S21†).[54] The result shows that after 48 h of incubation with 600 μg mL^{-1} N,S-CDs, the cell viability is still over 80%. Thus we can safely use 100 μg mL^{-1} N,S-CDs to incubate with HeLa cells for cell imaging. After 2 h of incubation at 37 °C with 5% CO_2, the cells are brightly illuminated and retain good morphologies under the confocal laser scanning microscope. These CDs are mainly located in the cytoplasm and they emit multicolor fluorescence under a laser of different wavelengths (Fig. 8), which further confirms the merits of our N,S-CDs.

4. Conclusions

Three kinds of CDs were synthesized, respectively, through the same route for comparison. These CDs had a similar particle size but different PLs and QYs. The N,S-CDs had the highest QY owing to the synergistic effect of nitrogen–sulfur co-doping. The optimal N,S-CDs showed excellent fluorescence stability, tunable emission color, high QY and low cytotoxicity, which ensured their successful application in Fe^{3+} ion detection and multicolor cell imaging. Our present research confirms that both functional groups on the surface of CDs and aromatic structures in the cores of CDs, especially the C=N bonds, are very essential to improve photoluminescence properties of carbon dots.

Acknowledgements

This work was supported by the National Major Basic Research Program of China (2013CB934101), the National Natural Science Foundation of China (21271045) and NCET-11-0115.

Notes and references

1 S. N. Baker and G. A. Baker, *Angew. Chem., Int. Ed.*, 2010, **49**, 6726.
2 H. Li, Z. Kang, Y. Liu and S. T. Lee, *J. Mater. Chem.*, 2012, **22**, 24230.
3 R. Liu, D. Wu, S. Liu, K. Koynov, W. Knoll and Q. Li, *Angew. Chem., Int. Ed.*, 2009, **48**, 4598.
4 S. Liu, J. Tian, L. Wang, Y. Luo, J. Zhai and X. Sun, *J. Mater. Chem.*, 2011, **21**, 11726.

5 H. Li, X. He, Z. Kang, H. Huang, Y. Liu, J. Liu, S. Lian, C. H. Tsang, X. Yang and S. T. Lee, *Angew. Chem., Int. Ed.*, 2010, **49**, 4430.
6 X. Xu, R. Ray, Y. Gu, H. J. Ploehn, L. Gearheart, K. Raker and W. A. Scrivens, *J. Am. Chem. Soc.*, 2004, **126**, 12736.
7 G. Eda, Y. Y. Lin, C. Mattevi, H. Yamaguchi, H. A. Chen, I. S. Chen, C. W. Chen and M. Chhowalla, *Adv. Mater.*, 2010, **22**, 505.
8 S. Qu, X. Wang, Q. Lu, X. Liu and L. Wang, *Angew. Chem., Int. Ed.*, 2012, **51**, 12215.
9 Y. P. Sun, B. Zhou, Y. Lin, W. Wang, K. A. S. Fernando, P. Pathak, M. J. Meziani, B. A. Harruff, X. Wang and H. Wang, *J. Am. Chem. Soc.*, 2006, **128**, 7756.
10 S. Zhu, Q. Meng, L. Wang, J. Zhang, Y. Song, H. Jin, K. Zhang, H. Sun, H. Wang and B. Yang, *Angew. Chem., Int. Ed.*, 2013, **52**, 3953.
11 S. Liu, J. Tian, L. Wang, Y. Zhang, X. Qin, Y. Luo, A. M. Asiri, A. O. Al-Youbi and X. Sun, *Adv. Mater.*, 2012, **24**, 2037.
12 Z. L. Wu, M. X. Gao, T. T. Wang, X. Y. Wan, L. L. Zheng and C. Z. Huang, *Nanoscale*, 2014, **6**, 3868.
13 W. Kwon, S. Do, J. Lee, S. Hwang, J. K. Kim and S. W. Rhee, *Chem. Mater.*, 2013, **25**, 1893.
14 X. Gao, Y. Cui, R. M. Levenson, L. W. Chung and S. Nie, *Nat. Biotechnol.*, 2004, **22**, 969.
15 I. L. Medintz, H. T. Uyeda, E. R. Goldman and H. Mattoussi, *Nat. Mater.*, 2005, **4**, 435.
16 C. Zhu, J. Zhai and S. Dong, *Chem. Commun.*, 2012, **48**, 9367.
17 S. Sahu, B. Behera, T. K. Maiti and S. Mohapatra, *Chem. Commun.*, 2012, **48**, 8835.
18 D. Sun, R. Ban, P. H. Zhang, G. H. Wu, J. R. Zhang and J. J. Zhu, *Carbon*, 2013, **64**, 424.
19 Z. L. Wu, P. Zhang, M. X. Gao, C. F. Liu, W. Wang, F. Leng and C. Z. Huang, *J. Mater. Chem. B*, 2013, **1**, 2868.
20 Y. Q. Zhang, D. K. Ma, Y. Zhuang, X. Zhang, W. Chen, L. L. Hong, Q. X. Yan, K. Yu and S. M. Huang, *J. Mater. Chem.*, 2012, **22**, 16714.
21 Z. Qian, J. Ma, X. Shan, H. Feng, L. Shao and J. Chen, *Chem. – Eur. J.*, 2014, **20**, 2254.
22 D. Qu, M. Zheng, L. Zhang, H. Zhao, Z. Xie, X. Jing, R. E. Haddad, H. Fan and Z. Sun, *Sci. Rep.*, 2014, **4**, 5294.
23 S. Chandra, P. Patra, S. H. Pathan, S. Roy, S. Mitra, A. Layek, R. Bhar, P. Pramanik and A. Goswami, *J. Mater. Chem. B*, 2013, **1**, 2375.
24 Y. Dong, H. Pang, H. B. Yang, C. Guo, J. Shao, Y. Chi, C. M. Li and T. Yu, *Angew. Chem., Int. Ed.*, 2013, **52**, 7800.
25 J. Deng, Q. Lu, N. Mi, H. Li, M. Liu, M. Xu, L. Tan, Q. Xie, Y. Zhang and S. Yao, *Chem. – Eur. J.*, 2014, **20**, 4993.
26 D. Pan, J. Zhang, Z. Li and M. Wu, *Adv. Mater.*, 2010, **22**, 734.
27 H. Ding, P. Zhang, T. Y. Wang, J. L. Kong and H. M. Xiong, *Nanotechnology*, 2014, **25**, 205604.
28 M. Zheng, Z. Xie, D. Qu, D. Li, P. Du, X. Jing and Z. Sun, *ACS Appl. Mater. Interfaces*, 2013, **5**, 13242.
29 R. Ye, C. Xiang, J. Lin, Z. Peng, K. Huang, Z. Yan, N. P. Cook, E. L. Samuel, C. C. Hwang, G. Ruan, G. Ceriotti, A. R. Raji, A. A. Marti and J. M. Tour, *Nat. Commun.*, 2013, **4**, 2943.
30 M. X. Gao, C. F. Liu, Z. L. Wu, Q. L. Zeng, X. X. Yang, W. B. Wu, Y. F. Li and C. Z. Huang, *Chem. Commun.*, 2013, **49**, 8015.
31 H. Nie, M. Li, Q. Li, S. Liang, Y. Tan, L. Sheng, W. Shi and S. X.-A. Zhang, *Chem. Mater.*, 2014, **26**, 3104.
32 D. M. Wang, M. X. Gao, P. F. Gao, H. Yang and C. Z. Huang, *J. Phys. Chem. C*, 2013, **117**, 19219.
33 W. Li, Z. Zhang, B. Kong, S. Feng, J. Wang, L. Wang, J. Yang, F. Zhang, P. Wu and D. Zhao, *Angew. Chem., Int. Ed.*, 2013, **52**, 8151.
34 J. Zhou, Y. Yang and C. Y. Zhang, *Chem. Commun.*, 2013, **49**, 8605.
35 M. J. Bojdys, J. O. Muller, M. Antonietti and A. Thomas, *Chem. – Eur. J.*, 2008, **14**, 8177.
36 Z. Yang, Z. Yao, G. Li, G. Fang, H. Nie, Z. Liu, X. M. Zhou, X. A. Chen and S. M. Huang, *ACS Nano*, 2012, **6**, 205.
37 Y. Deng, D. Zhao, X. Chen, F. Wang, H. Song and D. Shen, *Chem. Commun.*, 2013, **49**, 5751.
38 B. X. Zhang, H. Gao and X. L. Li, *New J. Chem.*, 2014, **38**, 4615.
39 Y. Wang and A. Hu, *J. Mater. Chem. C*, 2014, **2**, 6921.
40 M. J. Krysmann, A. Kelarakis, P. Dallas and E. P. Giannelis, *J. Am. Chem. Soc.*, 2012, **134**, 747.
41 Z. Q. Xu, L. Y. Yang, X. Y. Fan, J. C. Jin, J. Mei, W. Peng, F. L. Jiang, Q. Xiao and Y. Liu, *Carbon*, 2014, **66**, 351.
42 H. Tao, K. Yang, Z. Ma, J. Wan, Y. Zhang, Z. Kang and Z. Liu, *Small*, 2011, **8**, 281.
43 Y. Wang, S. Kalytchuk, Y. Zhang, H. Shi, S. V. Kershaw and A. L. Rogach, *J. Phys. Chem. Lett.*, 2014, **5**, 1412.
44 S. Zhu, J. Zhang, S. Tang, C. Qiao, L. Wang, H. Wang, X. Liu, B. Li, Y. Li, W. Yu, X. Wang, H. Sun and B. Yang, *Adv. Funct. Mater.*, 2012, **22**, 4732.
45 H. Zheng, Q. Wang, Y. Long, H. Zhang, X. Huang and R. Zhu, *Chem. Commun.*, 2011, **47**, 10650.
46 X. Wen, P. Yu, Y. R. Toh, X. Ma and J. Tang, *Chem. Commun.*, 2014, **50**, 4703.
47 S. L. Hu, K. Y. Niu, J. Sun, J. Yang, N. Q. Zhao and X. W. Du, *J. Mater. Chem.*, 2009, **19**, 484.
48 J. Liang, Y. Jiao, M. Jaroniec and S. Z. Qiao, *Angew. Chem., Int. Ed.*, 2012, **51**, 11496.
49 S. A. Wohlgemuth, R. J. White, M. G. Willinger, M. M. Titirici and M. Antonietti, *Green Chem.*, 2012, **14**, 1515.
50 D. Qu, M. Zheng, P. Du, Y. Zhou, L. Zhang, D. Li, H. Tan, Z. Zhao, Z. Xie and Z. Sun, *Nanoscale*, 2013, **5**, 12272.
51 K. Qu, J. Wang, J. Ren and X. Qu, *Chem. – Eur. J.*, 2013, **19**, 7243.
52 T. Lai, E. Zheng, L. Chen, X. Wang, L. Kong, C. You, Y. Ruan and X. Weng, *Nanoscale*, 2013, **5**, 8015.
53 C. Hu, C. Yu, M. Li, X. Wang, J. Yang, Z. Zhao, A. Eychmuller, Y. P. Sun and J. Qiu, *Small*, 2014, DOI: 10.1002/smll.201401328.
54 H. Ding, L. W. Cheng, Y. Y. Ma, J. L. Kong and H. M. Xiong, *New J. Chem.*, 2013, **37**, 2515.